Twinning and detwinning mechanisms in a BCC Ti Mo-Fe multilayered alloy

2017 IOP Conf. Ser.: Mater. Sci. Eng. 219 012042

(http://iopscience.iop.org/1757-899X/219/1/012042)

IOP Conf. Series: Materials Science and Engineering **219** (2017) 012042 doi:10.1088/1757-899X/219/1/012042

Twinning and detwinning mechanisms in a BCC Ti Mo-Fe multilayered alloy

I Gutierrez-Urrutia[1*], C-L Li[1], S Emura[1] and K Tsuchiya[1, 2]

[1] National Institute for Materials Science, Sengen 1-2-1, Tsukuba, Ibaraki, Japan
[2] Graduate School of Pure and Applied Sciences, University of Tsukuba, Ibaraki, Japan

*corresponding author e-mail: gutierrezurrutia.Ivan@nims.go.jp

Abstract. We have investigated {332}<113> twinning and detwinning mechanisms in a multilayered Ti-10Mo-xFe (x =1–3) alloy fabricated by multi-pass hot rolling. A strong influence of the Fe-graded structure on both phenomena is observed. The propagation of twins that are nucleated in Fe-lean regions (~1 wt.% Fe) is interrupted in the grain interiors at about 2 wt% Fe. We ascribe this effect to the role of the Fe content on the stress for twin propagation. The unusual twin structure determines the subsequent detwinning process upon thermal annealing. This process consists of two independent detwinning events that occur at two different microstructural regions, namely at twin tips located at grain interiors and at grain boundaries. Both detwinning modes can be explained from a thermodynamic standpoint whereby the boundary dissociation processes minimize the boundary free energy.

1. Introduction

In the last decade, β-Ti-Mo alloys have received considerable attraction as structural materials in several technological areas including the aerospace, automotive and biomedical industries. These alloys exhibit an outstanding combination of high specific strength, low elastic modulus and excellent bio-compatibility [1-6]. From an engineering standpoint, several processing techniques such as rolling, drawing and forging are typically used to optimize their mechanical behavior. For instance, Min et al. [6] have recently processed a multilayered bcc-Ti-10Mo-xFe (x= 1-3 wt.%) alloy by multi-pass hot rolling that exhibits a superior combination of strength and ductility (yield strength of 800 MPa; total elongation of 28%), compared to those of the individual alloys. This material contains a macroscopic gradient in Fe that tailors the combination of specific deformation mechanisms, namely <111> dislocation slip [7-9] and {332}<113> deformation twinning [10-12], resulting in superior mechanical behavior.

The activation of deformation modes in β-Ti-Mo alloys is associated with the stability of the β-Ti (bcc phase) compared to the β-α′ and β-α″ stress-induced phase transformation [13-15]. In bcc-stable β-Ti-Mo alloys the propagation of {332}<113> twins play an important role on the strain-hardening behaviour. The influence of microstructure on twin propagation is a complex phenomenon due to the different types of interfaces that exist in the microstructure (grain boundaries and twin interfaces), resulting in complex twin-interface interaction phenomena [16-21]. On the other hand, multilayered materials contain another microstructural feature that also influences twin propagation, namely, a chemical graded structure. The propagation of twins through a composition gradient may be

different to that occurring in homogeneous alloys due to solute effects on twinning [10, 11, 16, 18-20]. Another relevant feature of twinning is the thermal and mechanical stability of twin interfaces upon thermal annealing, including strain path reversion at room/high deformation temperature or under specific stress states. This phenomenon is associated with the thermal and mechanical stability of twin interfaces, which is controlled by the twin interface structure [16, 21, 22]. In bcc metals, the detwinning mechanism has hardly been analyzed [23] in spite of the large number of reports on {112}<111> and {332}<113> twinning modes [11, 16, 24, 25]. The present work aims at investigating different aspects of {332}<113> twinning and detwinning in a multilayered β-Ti-10Mo-xFe (x: 1-3). We investigate the propagation behaviour of twins through the Fe-graded structure and the detwinning behaviour upon thermal annealing at 900°C. Twin and detwin structures are characterized by electron backscatter diffraction (EBSD) and electron channeling contrast imaging (ECCI).

2. Experimental procedure

The material investigated in this work was a multilayered material consisting of ten alternating layers of Ti-10Mo-1Fe and Ti-10Mo-3Fe (wt.%) alloys. The material was fabricated by multi-pass hot rolling at 1000 °C from individual layers of about 3.5 mm in thickness, and was subsequently solution treated at 900 °C for 1 hour followed by water quenching. Details of the processing procedure are described in [7]. The final thickness of the as-processed 10-layer material was about 2.7 mm. Tensile samples were machined from the multilayered material and from individual alloy sheets, namely, Ti-10Mo-1Fe, Ti-10Mo-2Fe and Ti-10Mo-3Fe. The tensile samples had an 18 mm gage length, a 4 mm gage width and a 2.5 mm gage thickness. The tensile axis was parallel to the rolling direction (RD). The detwinning process was investigated in samples annealed at 900 °C for 60 and 90 seconds in air followed by water quenching, as suggested by a former study [23]. Tensile tests were performed in an Instron 5581 tensile machine at room temperature and at an initial strain rate of $1 \times 10^{-5}\ s^{-1}$. Twin and detwin structures were examined on the longitudinal section defined by the tensile direction (TD) and normal direction (ND). Microstructural characterization was performed using two electron microscopy techniques, namely, electron channeling contrast imaging (ECCI) and electron backscatter diffraction (EBSD) in a Sigma Zeiss field emission gun scanning electron microscope (FEG-SEM) equipped with a backscattering electron detector (BSE) and a TSL orientation imaging microscopy (OIM) EBSD system. ECC images were obtained with optimum channeling contrast following the procedure described in [26]. ECCI was carried out at a working distance of 4 - 5 mm and at 9 kV accelerating voltage using an aperture size of 120 μm. EBSD maps were taken at 20 kV accelerating voltage, a working distance of 15 mm and with step sizes ranging between 100 nm and 2 μm. Elemental mapping was performed using electron probe microanalysis (EPMA) on a JEOL JXA-8900F system operated at 15 kV.

3. Results and discussion

Figure 1 shows the deformation microstructure (a) and the elemental distribution (b) of the multilayered material tensile-deformed to a true strain of 0.04. The elemental map shows that the multilayered alloy contains a macroscopic gradient of Fe, ranging between 1 and 3 wt%, distributed in the form of bands parallel to the RD. The Ti and Mo are homogeneously distributed within the Fe-graded structure [28]. The Fe-graded bands are about 130 μm thick and are situated between the original 1 wt.%Fe and 3 wt.%Fe layers, which are about 50 μm thick.

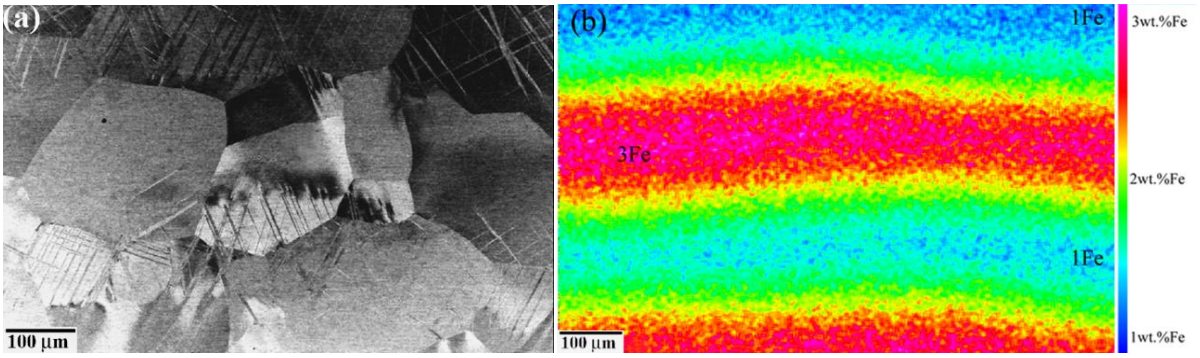

Figure 1. (a) ECC image of the deformation structure of the multilayered Ti-10Mo-xFe (x = 1–3) material tensile deformed to 0.04 true strain. (b) EPMA map showing the Fe distribution [27].

Figure 2(a) shows an example of the deformation structure of a grain oriented close to the [1 15 16] crystallographic direction. The figure reveals that the deformation structure is formed by {332}<113> deformation twins and by <111> slip traces. This structure is similar to that reported in conventional (chemically homogeneous) β-Ti-Mo alloys [9, 10]. However, in the present multilayered Ti-Mo-Fe alloy the propagation of deformation twins is interrupted within the grain interiors. In particular, in the grain shown in figure 2(a) twins are nucleated at the grain boundary GB1 (TN: twin nucleation) and are interrupted in the grain interior at about 1.8 wt% Fe (TT: twin tip). Elemental mapping reveals that the grain contains a Fe gradient of about of about 0.01 wt% Fe/µm over a region 160 µm long. The Fe content varies between 1.2 wt% (at the grain boundary, GB1) and 2.8 wt% (at the low angle grain boundary marked LAGB2). In the same area the Mo content is relatively homogeneous and ranges between 9.8 and 10.2 wt%. The EPMA line analysis in figure 2(b) shows that the Fe variation within the graded structure is smooth, i.e. no sharp homophase interface occurs. Interestingly, under the current thermomechanical conditions, the role of precipitates such as ω-omega phase, on the precipitate-twin interaction can be ruled out due to their small volume fraction (<0.01) and their shearable nature [28]. These observations indicate that the variation in Fe content is the main microstructural parameter controlling twin propagation.

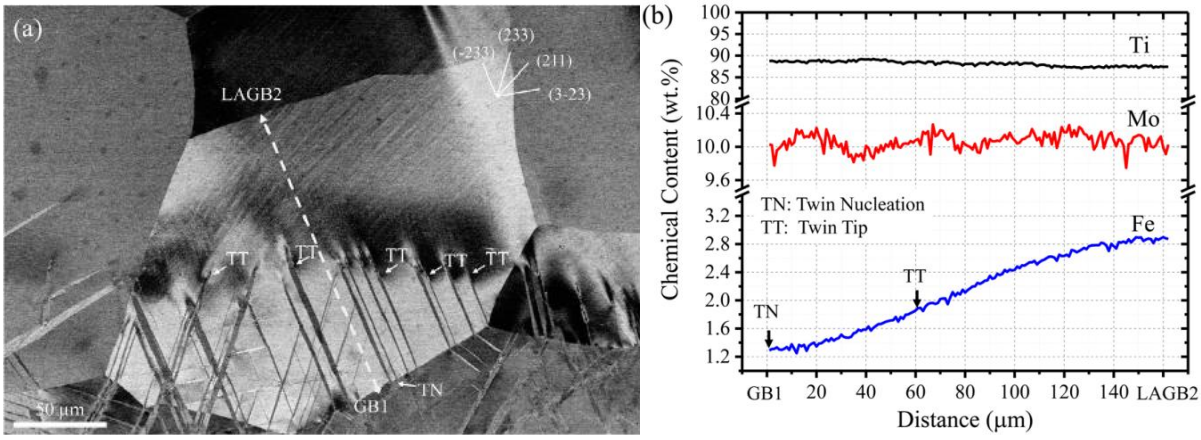

Figure 2. (a) ECC image of the deformation structure of a grain oriented close to [1 15 16]; (b) chemical line analysis performed by EPMA along the dashed line within the grain shown in (a). TN: twin nucleation; TT: twin tip; GB: grain boundary; LAGB: low angle grain boundary [28].

As the processed material does not contain any sharp interface between chemical layers, due to the evolution of the original layer interfaces into migrating grain boundaries, we assume an iso-stress condition for the in-grain propagation of twins. In order to clarify the role of Fe content on twin

propagation, we have experimentally determined the twinning stress, σ_{tw}, of the Ti-10Mo-xFe (x = 1–3) system. We define σ_{tw} as the macroscopic stress at which twins are detected. According to dislocation-based models of twinning in bcc metals, the experimental twinning stress corresponds to the stress to grow an existing twin nucleus [16, 19, 20, 25]. Specifically, σ_{tw} for each of the three individual alloys, namely Ti-10Mo-1Fe, Ti-10Mo-2Fe and Ti-10Mo-3Fe (wt.%), was determined by tensile loading experiments. The alloys contained similar average grain sizes of ~250 μm in order to avoid any grain-size effects on the twinning stress. In the alloys with lower Fe content, i.e. Ti-10Mo-1Fe and Ti-10Mo-2Fe, {332}<113> twins readily formed at yielding. For these alloys we thus consider the twin stress to equal the yield stress. In contrast, deformation twins were not visible in the Ti-10Mo-3Fe alloy at any investigated strain level. Accordingly, we can only estimate a lower bound of the twinning stress for this alloy system. The experimental values of the twin stress as a function of Fe content are plotted in figure 3.

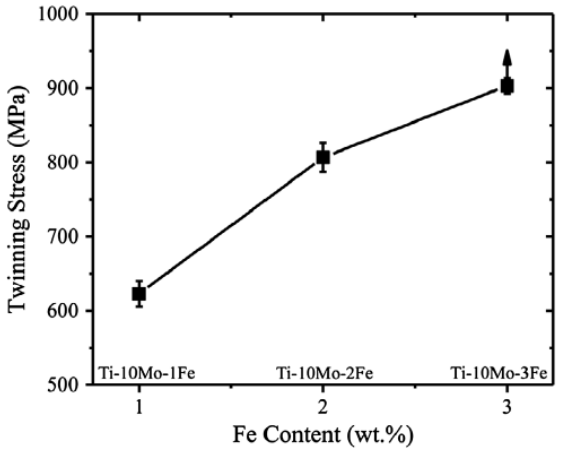

Figure 3. Effect of Fe content on the twinning stress in the Ti-10Mo alloy system. Error bars indicate the experimental deviation [27].

Figure 3 shows that twinning stress increases with Fe content. Specifically, we observe that additions of Fe higher than 1 wt% promote a significant increase of the twinning stress, namely, 2 wt% Fe increases the twinning stress about 205 MPa, and 3 wt% Fe increases the twinning stress at least 330 MPa compared with the 1 wt% addition. These findings indicate that the stress to propagate a twin plate nucleated in a Fe-lean region and propagating through a Fe-graded structure increases significantly with the propagation distance. For the graded alloy in the present study the deformation conditions are such that the macroscopic applied stress is about 830 MPa, which is slightly higher than the twinning stress for the Ti-10Mo-2Fe alloy (σ_{tw} = 780 MPa). This result indicates that twins nucleated in the Fe-lean region (~1 wt% Fe) are able to propagate within the interior of a grain up to an area containing about 2 wt% Fe, which is close to the experimentally observed value of 1.8 wt% Fe.

{332}<113> detwinning was also investigated using EBSD in a grain oriented favorably for deformation twinning, namely the [-13 14 5] crystallographic direction (Schmid factor, SF, for twinning of 0.49), see figure 4. At a true strain of 0.04 (figure 4a) the grain contains two active twin systems, namely (3-32) [1-1-3] and (233) [-311], which correspond to the twin systems with the highest Schmid factors (SF = 0.49 and SF = 0.3, respectively). Due to the negligible volume fraction of secondary twins, we have only analyzed the detwinning mechanism of primary twins, i.e., the (3-32) [1-1-3] system. Figure 4(b,c) shows the further evolution of the twin structure after short annealing treatments at 900°C of either 60 s (figure 4b) or 90 s (figure 4c). The IPF-EBSD maps show that detwinning is characterized by the gradual detachment of the twinned volumes from grain boundaries (GB) and also show the evolution of the boundaries that form the twin tip (TT) into a single twin boundary. These results indicate that the unusual deformation twin structure of the present

multilayered material (figure 2) determines the detwinning behaviour, which is characterized by two independent events occurring at different microstructural regions, namely twin tips (TT) located in grain interiors and at grain boundaries (GB).

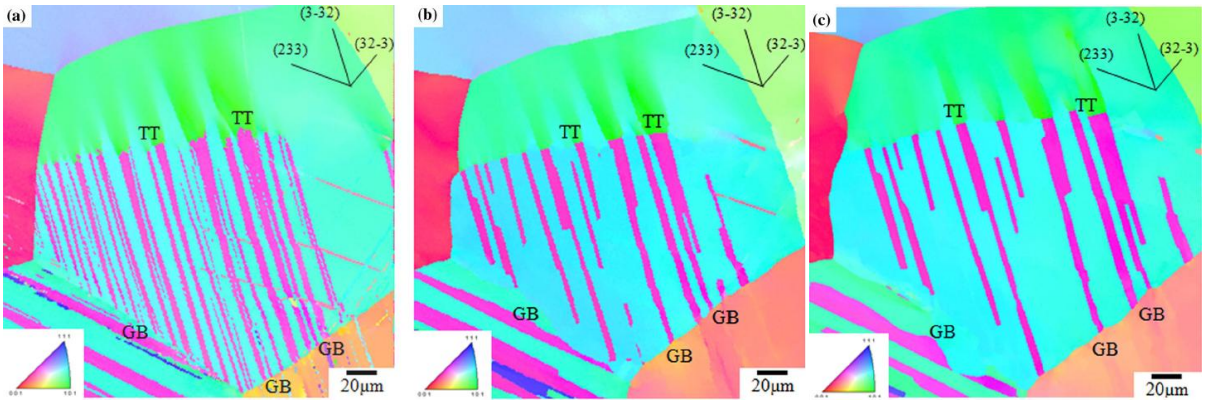

Figure 4. IPF-EBSD maps colored according to the tensile axis direction showing the evolution of the {332}<113>twin structure with annealing time at 900 °C in a grain with [-13 14 5] crystallographic direction; (a) deformation twin structure at 0.04 true strain; (b) detwinned structure at 900 °C/60 s; (c) detwinned structure at 900 °C/90 s. (GB grain boundary; TT twin tip.) [29]

Figures 5(a,b) show the evolution of the detwinning process occurring at twin tips in more detail. The underlying boundary reactions were analyzed by EBSD. Twin crystals are delimited by coherent twin boundaries (CTBs), characterized as twin boundaries with angle/rotation axis pair of 50.5°/<110>. Twin tips are formed by incoherent twin boundaries (ITBs), which are characterized as twin boundaries with angle/rotation axis pair of 60°/<110>, figure 5(a). Upon annealing at 900°C for 60 s, ITBs evolve into a single Σ3 boundary that is characterized by an angle/rotation axis pair of 70.3°/<110>, figure 5(b). The evolution of a high angle grain boundary into a Σ3 boundary has been frequently observed in [110]-misoriented tilt boundaries, such as Σ11 boundaries, in fcc metals [21, 30]. The process can be explained from a thermodynamic standpoint since the reaction process Σ11 → Σ3 minimizes the overall boundary free energy. In the present detwinning event, the driving force for the subsequent mobility of the Σ3 boundaries upon thermal annealing is the stored energy of plastic deformation localized around the twin tips [27].

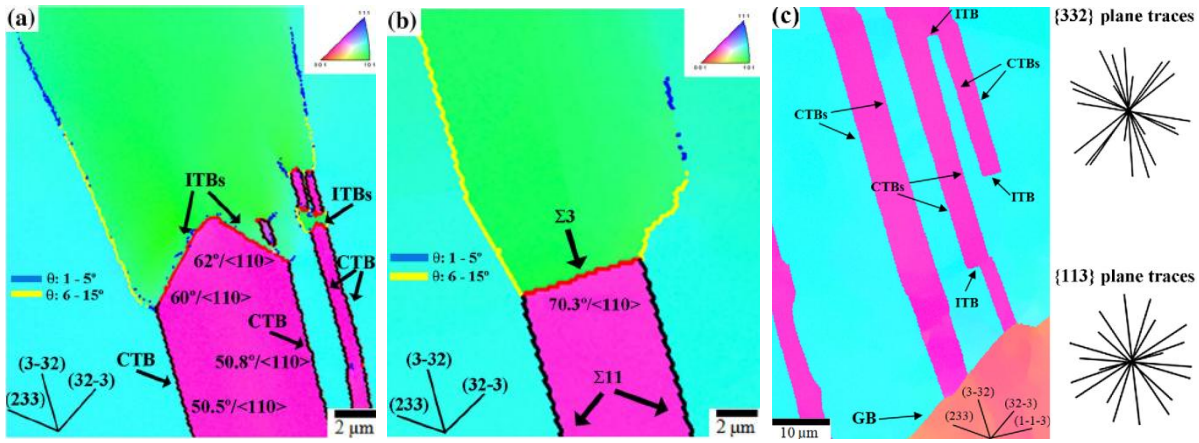

Figure 5. Evolution of the {332}<113> detwinning process at twin tips. (a) Deformation twin structure at 0.04 true strain. (b) Detwinned structure at 900 °C/60 s. (c) Detwinning process at a grain boundary upon annealing treatment of 900 °C/90 s. θ indicates misorientation angle; GB grain boundary; CTB coherent twin boundary; ITB incoherent twin boundary.

Figure 5(c) shows details of the detwinning events occurring at grain boundaries. Specifically, this figure shows the detwinned structure close to a grain boundary after annealing 900°C for 90 s. It can be seen that detwinning process is characterized by the detachment of the twinned volumes from grain boundaries by the formation and migration of incoherent twin boundaries (ITBs) that are perpendicular to the existing Σ11 {332} CTBs, as revealed by plane trace analysis. Crystallographic analysis by EBSD reveals that ITBs correspond to Σ11 {113} incoherent twin boundaries that are characterized by an angle/rotation axis pair of 50.5°/<110>. The detwinning process occurring at grain boundaries can also be explained from a thermodynamic standpoint where the boundary dissociation process minimizes the overall boundary free energy [21,31,32]. Recent calculations of grain boundary energies in bcc metals (Fe and Mo) by the embedded atom method have shown that Σ11 {113} is a low energy grain boundary [31, 32] and hence, its formation reduces the grain boundary free energy. Thermal energy triggers the subsequent migration of ITBs resulting in the formation of large-scaled facets in the twin interface structure upon thermal annealing, as seen in figure 5(c).

The present results indicate that the detwinning process occurring at grain boundaries is controlled by the formation and migration of Σ11 {113} ITBs, which leads to the formation of large facets in the detwinned structure that are perpendicular to the existing CTBs. It is worth commenting that the geometry of the detwinned structure observed in the present bcc-TiMoFe alloy is similar to that commonly observed in fcc metals consisting of Σ3 {111} CTBs containing perpendicular facets formed by Σ3 {112} ITBs [21, 30, 33, 34]. In fcc metals, Σ3 {112} ITBs are represented by a set of Shockley partial dislocations on every {111} plane with a repeatable sequence b_2:b_1:b_3 (where b_i represents the Burgers vector of the Shockley partials) and where the sum of the Burgers vectors in each unit set of three planes equals zero. However, as the crystal defect configurations of Σ11 {332} CTB and Σ11 {113} ITB are still unknown [10–12] we cannot perform a sound analysis of the {332}<113> detwinning structure. Further work is required to elucidate this relevant point. Interestingly, the role of ITBs on the twinning and detwinning processes in fcc metals such as coarse grained, nanocrystalline and sputtered thin films has been recently addressed [33,34]. These works suggest that the formation and migration of ITBs control the kinetics of detwinning. The present results also underline the key role of ITBs on the detwinning of {332}<113> twins in bcc–Ti–Mo alloys and, in particular, on the detachment of twins from grain boundaries. Further work is, however, required to understand the mechanism of formation and migration of {113} ITBs in bcc–Ti–Mo alloys.

4. Conclusions

We have investigated using EBSD and ECCI the propagation and detwinning behavior of {332}<113> twins in a multilayered Ti-10Mo-xFe (x = 1–3) alloy fabricated by multi-pass hot rolling. We observe that the Fe-graded structure has a significant influence on both phenomena. The propagation of twins that are nucleated at grain boundaries in Fe-lean regions (~1 wt% Fe) is interrupted in the grain interior at an Fe concentration of about 2 wt%. We ascribe this effect to the strong influence of the Fe content on the stress for twin propagation. Additionally, it is found that the detwinning process upon thermal annealing consists of two independent detwinning modes that occur in two different microstructural regions, namely twin tips located in grain interiors and at grain boundaries. The first detwinning mode is characterized by the evolution of incoherent twin boundaries (ITBs) into a Σ3 boundary followed by subsequent migration of the Σ3 boundary. The second detwinning process is characterized by the detachment of twin volumes from a grain boundary by the formation and migration of Σ 11 {113} incoherent twin boundaries (ITBs). Both detwinning modes can be explained from a thermodynamic standpoint whereby the observed boundary dissociation processes minimize the boundary free energy.

Acknowledgments

The authors wish to acknowledge financial support from NIMS.

References

[1] Niinomi M 2008 *J. Mech. Beh. Biom. Met.* **1** 30
[2] Al-Zain Y, Sato Y, Kim HY, Hosoda H, Nam TH and Miyazaki S 2012 *Acta Mater.* **60** 2437
[3] Geetha M, Singh AK, Asokamani R and Gogia AK 2009 *Prog. Mater. Sci.* **54** 397
[4] Banerjee D and Williams JC 2013 *Acta Mater.* **61** 844
[5] Clément N, Lenain A and Jacques PJ 2007 *JOM* **59** 50
[6] Min XH, Emura S, Meng FQ, Mi GB and Tsuchiya K 2015 *Scripta Mater*. **102** 79
[7] Christian JW 1983 *Metall. Trans.* **14A** 1237
[8] Taylor G 1992 *Prog. Mater. Sci.* **36** 29
[9] Lee SH, Hagihara K and Nakano T 2012 *Metall. Mater. Trans. A* **43** 1588
[10] Kawabata T, Kawasaki S and Izumi O 1998 *Acta Mater.* **46** 2705
[11] Tobe H, Kim HY, Inamura T, Hosoda H and Miyazaki S 2014 *Acta Mater.* **64** 345
[12] Rusakov GM, Litvinov AV and Litvinov VS 2006 *Met. Sci. Heat. Treat.* **48** 244
[13] Hida M, Sukedai E, Henmi C, Sakaue K and Terauchi H 1982 *Acta Metall.* **30** 1471
[14] Ohyama H and Nishimura T 1995 *ISIJ Int.* **35** 927
[15] Hanada S, Takemura A and Izumi O 1982 *Trans. Jpn. Inst. Met.* **23** 507
[16] Christian JW and Mahajan S 1995 *Prog. Mater. Sci.* **39** 1
[17] Steinmetz DR, Jäpel T, Wietbrock B, Eisenlohr P, Gutierrez-Urrutia I, Saeed-Akbari A, Hickel T, Roters F and Raabe D 2013 *Acta Mater.* **61** 494
[18] Gutierrez-Urrutia I, Zaefferer S and Raabe D 2010 *Mater. Sci. Eng. A* **527** 3552
[19] Mahajan S and Williams DF 1973 *Int. Metall. Rev.* **18** 43
[20] Meyers MA, Vöhringer O and Lubarda VA 2001 *Acta Mater.* **49** 4025
[21] Sutton AP and Balluffi RW 1995 *Interfaces in Crystalline Materials* (Oxford, Oxford University Press)
[22] Wang YM, Sansoz F, LaGrange T, Ott RT, Marian J, Barbee TW and Hamza AV 2013 *Nature Mater.* **12** 697
[23] Qu L, Yang Y, Lu YF, Feng L, Hu JH, Ge P, Zhou W, Han D and Ping DH 2013 *Scripta Mater.* **69** 389
[24] Lai MJ, Tasan CC and Raabe D 2016 *Acta Mater.* **111** 173
[25] Narita N and Takamura JI 1992 Deformation twinning in f.c.c. and b.c.c. metals *Dislocations in Solids* (vol 9 Dislocations and Disclinations) ed Nabarro F R N (Amsterdam, North-Holland) p 135
[26] Gutierrez-Urrutia I, Zaefferer S and Raabe D 2013 *JOM* **65** 1229
[27] Gutierrez-Urrutia I, Li C-L, Min X, Emura S and Tsuchiya K 2016 *STAM* **17** 220
[28] Banerjee S and Naik UM 1996 *Acta Mater.* **44** 3667
[29] Gutierrez-Urrutia I, Li C-L and Tsuchiya K 2017 *J. Mater. Sci*. **52** 7858
[30] Goodhew PJ, Tan TY and Balluffi RW 1978 *Acta Metall.* **26** 557
[31] Tschopp MA, Solanki KN, Gao F, Sun X, Khaleel MA and Horstemeyer MF 2012 *Phys. Rev. B* **85** 064108
[32] Ratanaphan S, Olmsted DL, Bulatov VV, Holm EA, Rollett AD and Rohrer GS 2015 *Acta Mater*. **88** 346
[33] Wang J, Li N, Anderoglu O, Zhang X, Misra A, Huang JY and Hirth JP 2010 *Acta Mater.* **58** 2262
[34] Velasco L and Hodge AM 2016 *Acta Mater.* **109** 142